Underwater Scene Reconstruction via Image Pre-processing

[*]Huimin Lu, Yujie Li and Xuelong Hu

Abstract

This paper describes a novel method for enhancing ocean optical images using weighted filter and spectral properties. While light is traveling through the water, light rays are distorted depending on the wavelength. Absorption, scattering and color distortion are three major distortion issues for underwater optical imaging. Scattering is caused by large suspended particles, as in turbid water that contains abundant particles, which causes the degradation of the captured image. Color distortion corresponds to the varying degrees of attenuation encountered by light traveling in water at different wavelengths, causing ambient underwater environments to be dominated by a bluish tone. Our key contributions proposed include a novel deep-sea imaging model to compensate for the attenuation discrepancy along the propagation path and an effective underwater scene reconstruction method. The recovered images are characterized by a reduced noised level, better exposure of the dark regions, and improved global contrast where the finest details and edges are enhanced significantly.

Keywords: deep-sea imaging; inherent optical properties; image reconstruction; ocean observation

*Corresponding Author: Huimin Lu
(E-mail: luhuimin@ieee.org).
[1] Kyushu Institute of Technology, Japan
[2] Yangzhou University, China

1. Introduction

With the development of exploring the deep-sea by autonomous underwater vehicles (AUVs) and unmanned underwater vehicles (UUVs), the resolution of underwater images remains as a major issue. That is, how to acquire a clear underwater image is a question. From the 1960s, sonar has been widely used for detection and recognition of objects in oceans. Because of acoustic imaging principle, the sonar imaged images have many shortcomings, such as the low signal to ratio, low resolution et al. Consequently, optical vision sensors must then be used instead for short-range identification because of the low quality of images restored by sonar imaging [1].

In contrast to normal images, underwater images suffer from poor visibility owing to the medium. The light is absorbed when sunlight is reflected by a water surface. Furthermore, light is also deflected and scattered by many particles in water. In addition, absorption substantially reduces the atmospheric light energy. The random attenuation of light primarily causes a hazy appearance, while the fraction of light scattered back from the water along the line of sight considerably degrades the scene contrast. In particular, objects at a distance of more than 10 meters are almost indistinguishable, because the colors are faded owing to the characteristic wavelengths that are filtered according to the water

depth [2]. Furthermore, a distinctive footprint of the light beam is typically left on the seafloor when an artificial light source is employed.

In the last decade, there are some researchers focused on underwater image quality improvement. Y.Y. Schechner et al. exploited a polarization imaging method to compensate for visibility degradation [3], while Ancuti et al. used an image fusion method in a turbid medium to reconstruct a clear image [4]. Hou et al. combined a point spread function and a modulation transfer function to reduce the effects of blurring [5]. Ouyang et al. proposed bilateral filtering based on an image deconvolution method [6]. Although the aforementioned approaches can enhance the image contrast, these methods have demonstrated several drawbacks that reduce their practical applicability. First, the equipment for imaging is difficult to use in practice (e.g., a range-gated laser imaging system, which is hardly applied in practice). Second, multiple input images are required [7]. Third, they cannot alleviate color distortion very well.

Instead of multiple input images, underwater scene reconstruction methods using a single image have been proposed. The ICA based on a dahazing method was first proposed by Fattal [8]. He estimated the scene radiance and derived the transmission image by a single image. However, this method cannot sufficiently process images with heavy haze. Then, He et al. [9] proposed a scene depth information-based dark channel prior a dehazing algorithm using a matting Laplacian. However, this algorithm requires significant computation time. To overcome this disadvantage, they also proposed a new guided image filter [10] with the foggy image

used as a reference image. However, this method leads to incomplete haze removal.

Hence, in this paper, we introduce a novel approach to enhance underwater images based on a single image to overcome the drawbacks of the conventional methods mentioned above. The organization of this paper is as follows. Section 2 explains the ocean imaging model. Section 3 describes the model for underwater image enhancement and proposes our guided trigonometric bilateral filter. Section 4 applies our proposed method for underwater optical images. Finally, Section 5 concludes this paper.

2. Underwater Imaging Model

Artificial light and atmospheric light traveling through the water is the source of illumination in an ocean environment. Let suppose the amount of radiation light W(x) formed after wavelength attenuation can be formulated according to the energy attenuation model as follows:

$$E_\lambda^W(x) = E_\lambda^A(x) \cdot Nrer(\lambda)^{D(x)} + E_\lambda^I(x) \cdot Nrer(\lambda)^{L(x)}, \quad (1)$$
$$\lambda \in \{r, g, b\}$$

where $E_\lambda^W(x)$ is the amount of illumination at point x, $E_\lambda^A(x)$ is the amount of illumination of atmospheric light at point x, $E_\lambda^I(x)$ is the illumination of artificial light, and *Nrer* is the normalized residual energy ratio. At the scene point x, artificial light reflected again travels distance $L(x)$ to the camera forming pixel $I_\lambda(x)$, $\lambda \in \{r, g, b\}$. $D(x)$ is the scene depth underwater. We suppose the absorption and scattering rate is $\rho(x)$, and artificial light $J_\lambda(x)$ emanated from point x is equal to the amount of illuminating ambient light $E_\lambda^W(x)$ reflected,

$$E_\lambda^W(x) = \left(E_\lambda^A(x) \cdot Nrer(\lambda)^{D(x)} + E_\lambda^I(x) \cdot Nrer(\lambda)^{L(x)}\right) \cdot \rho(x), \quad (2)$$
$$\lambda \in \{r,g,b\}$$

By following the improved Nayar-Narasimhan hazing model [13], the image $I_\lambda(x)$ formed at the camera plane can be formulated as,

$$I_\lambda(x) = \left(E_\lambda^A(x) \cdot Nrer(\lambda)^{D(x)} + E_\lambda^I(x) \cdot Nrer(\lambda)^{L(x)}\right) \cdot t_\lambda(x) \qquad (3)$$
$$+ (1 - t_\lambda(x)) \cdot B_\lambda, \quad \lambda \in \{r,g,b\}$$

where the background B_λ represents the part of the object reflected light J_λ, and ambient light E_λ^W is scattered toward the camera by particles in the water. The residual energy ratio $t_\lambda(x)$ can be represented alternatively as the energy of a light beam with wavelength λ before and after traveling distance $d(x)$ within the water $E_\lambda^{residual}(x)$ and $E_\lambda^{initial}(x)$, respectively, as follows:

$$t_\lambda(x) = \frac{E_\lambda^{residual}(x)}{E_\lambda^{initial}(x)} = 10^{-\beta(\lambda)d(x)} = Nrer(\lambda)^{d(x)} \qquad (4)$$

where *Nrer* is the normalized residual energy ratio [14], in the Ocean Type I, it follows:

$$N_{rer}(\lambda) = \begin{cases} 0.8 \sim 0.85 & if \ \lambda = 650 \sim 750 \mu m(red) \\ 0.93 \sim 0.97 & if \ \lambda = 490 \sim 550 \mu m(green) \\ 0.95 \sim 0.99 & if \ \lambda = 400 \sim 490 \mu m(blue) \end{cases} \qquad (5)$$

Consequently, subscribing the Eq. (3) and Eq. (4), we can obtain:

$$I_\lambda(x) = \left[\left(E_\lambda^A(x) \cdot Nrer(\lambda)^{D(x)} + E_\lambda^I(x) \cdot Nrer(\lambda)^{L(x)}\right) \cdot \rho_\lambda(x)\right] \cdot Nrer(\lambda)^{d(x)}$$
$$+ \left(1 - Nrer(\lambda)^{d(x)}\right) \cdot B_\lambda, \quad \lambda \in \{r,g,b\} \qquad (6)$$

The above equation incorporates the light scattering during the course of propagation from object to the camera $d(x)$, and the wavelength attenuation along both the light-object path $L(x)$, scene depth $D(x)$ and object-camera path $d(x)$. Once the light-object distance $L(x)$, scene depth $D(x)$ and object-camera distance $d(x)$ are known, the final

clean image will be recovered. Figure 1 shows the diagrammatic sketch of the proposed model.
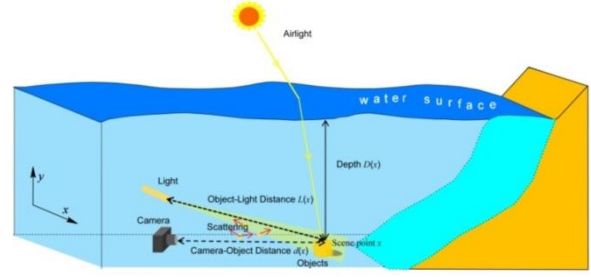
Figure 1: Diagram of Shallow Ocean Optical Imaging Model.

3. Underwater Image Improvement Methods

3.1 Absorption and Scattering Removal

In Ref. [19], the author found that the red color channel is the dark channel of underwater images. During our experiments, we found that the lowest channel of RGB channels in turbidly water is not always the red color channel; the blue color channel is very significant [25, 27]. The reason is that we usually take artificial light in imaging. Although the red wavelength is absorbed easily through traveling in water, the distance between the camera and an object is not enough to absorb the red wavelength significantly. The blue channel may be the lowest. Consequently, in this paper, we take the minimum pixel value as the rough depth disparity.

As mentioned in Eq. (6), light $J_\lambda(x)$ reflected from point x is

$$J_\lambda(x) = \left(E_\lambda^A(x) \cdot Nrer(\lambda)^{D(x)} + E_\lambda^I(x) \cdot Nrer(\lambda)^{L(x)}\right) \cdot \rho_\lambda(x),$$
$$\lambda \in \{r,b\} \qquad (7)$$

We define the minimum pixel channel $J_{dark}(x)$ for the underwater image $J_\lambda(x)$ as

$$J_{dark}(x) = \min_\lambda \min_{y \in \Omega(x)} J_\lambda(y), \lambda \in \{r,b\} \qquad (8)$$

If point x belongs to a part of the foreground object, the value of the minimum pixel channel is very small. Taking the min operation in the local patch $\Omega(x)$ on the scattered image $I_\lambda(x)$ in Eq. (6), we have

$$\min_{y \in \Omega(x)}(I_\lambda(y)) = \min_{y \in \Omega(x)}\left\{ J_\lambda(y) \cdot Nrer(\lambda)^{d(y)} + \left(1 - Nrer(\lambda)^{d(y)}\right) \cdot B_\lambda \right\}, \quad \lambda \in \{r,b\} \tag{9}$$

Since B_λ is the homogeneous background light and the residual energy ratio $Nrer(\lambda)^{d(y)}$ on the small local patch $\Omega(x)$ surrounding point x is essentially a constant $Nrer(\lambda)^{d(x)}$, the min value on the second item of Eq. (18) can be subsequently removed as

$$\min_{y \in \Omega(x)}(I_\lambda(y)) = \min_{y \in \Omega(x)}\left\{ J_\lambda(y) \cdot Nrer(\lambda)^{d(x)} + \left(1 - Nrer(\lambda)^{d(x)}\right) \cdot B_\lambda \right\}, \quad \lambda \in \{r,b\} \tag{10}$$

We rearrange the above equation and perform on the minimum operation among red and blue color channels as follows:

$$\min_\lambda\left\{\frac{\min_{y \in \Omega(x)}(I_\lambda(y))}{B_\lambda}\right\} = \min_\lambda\left\{\frac{\min_{y \in \Omega(x)} J_\lambda(y)}{B_\lambda} \cdot Nrer(\lambda)^{d(x)}\right\} + \min_\lambda\left(1 - Nrer(\lambda)^{d(x)}\right), \lambda \in \{r,b\} \tag{11}$$

Therefore, the second item of the above equation is the dark channel equal to 0. Consequently, the estimated depth map is

$$\min_\lambda\left(Nrer(\lambda)^{d(x)}\right) = 1 - \min_\lambda\left\{\frac{\min_{y \in \Omega(x)}(I_\lambda(y))}{B_\lambda}\right\}, \lambda \in \{r,b\} \tag{12}$$

Finally, the depth map can be obtained by,

$$d(x) = \ln\left(1 - \min_\lambda\left\{\frac{\min_{y \in \Omega(x)}(I_\lambda(y))}{B_\lambda}\right\}\right) / \ln Nrer(\lambda) \tag{13}$$

In this subsection, we propose a guided trigonometric bilateral filter (GTBF) to overcome the occurrence of gradient reversal artifacts. The filtering process of the GTBF is first performed under the guidance of image G that can be another image or the input image I itself. Let I_p and G_p be the intensity values at the pixel p of the minimum channel image and the guided image, respectively, and w_k be the kernel window centered at pixel k, consistent with the bilateral filter. GTBF is then formulated by,

$$GTBF(I)_p = \frac{1}{\sum_{q \in w_k} W_{GTBF_{pq}}(G)} \sum_{q \in w_k} W_{GTBF_{pq}}(G) I_q \tag{14}$$

where the kernel weight function $W(G)$ can be written by

$$W_{GTBF_{pq}}(G) = \frac{1}{|w|^2} \sum_{k:(p,q) \in w_k}\left(1 + \frac{(G_p - \mu_k)(G_q - \mu_k)}{\sigma_k^2 + \varepsilon}\right) \tag{15}$$

where μ_k and σ_k^2 are the mean and variance of the guided image G in the local window w_k, and $|w|$ is the number of pixels in this window. When both G_p and G_q are concurrently on the same side of an edge, the weight assigned to pixel q is large. When G_p and G_q are on different sides, a small weight will be assigned to pixel q.

According to Nayar-Narasimhan hazing model, we can obtain the descattered image by

$$\tilde{J}_\lambda(x) = \frac{I_\lambda(x) - \left(1 - Nrer(\lambda)^{d(x)}\right) \cdot B_\lambda}{Nrer(\lambda)^{d(x)}}$$
$$= E_\lambda^A(x) \cdot Nrer(\lambda)^{D(x)} \cdot \rho_\lambda(x) \cdot Nrer(\lambda)^{d(x)}, \quad \lambda \in \{r,g,b\} \tag{16}$$

(a)   (b)

(c)
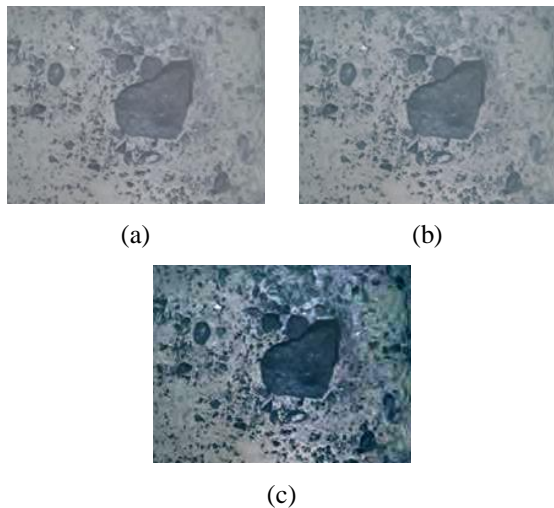
Figure 4: Simulation result of absorption and scattering removal. (a) Artificial light adjusted image; (b) Absorption corrected result; (c) De-scattered result.

3.2 3D Scene Reconstruction

In Ref. [31], the authors reconstruct the underwater scene by two cameras. In this paper, we recover the 3d scene by single camera. During de-scattering, we obtained the scene disparity map, and we also got the de-scattered image. Therefore, we can reconstruct the scene by [32].

4. Experiments and Discussions

The performance of the proposed algorithm is evaluated both objectively and subjectively by utilizing ground-truth color patches. Both results demonstrate superior haze removal and color balancing capabilities of the proposed method over the others. In the experiment, we compare our method with Schechner's model, Bazeille's model, Fattal's model, Nicholas's model, He's model, Xiao's model, Ancuti's model, and Chiang's model. Here,

we select the best parameters for each model. The computer used is equipped with Windows XP and an Intel Core 2 (2.0 GHz) with 1 GB RAM.

Figure 5 shows the results using different reconstruction methods. As first evaluation, the performance of the proposed method is compared with other methods in removing the haze-like objects in the water. Figure 4 illustrates this example using different dehazing methods. He et al.'s work [6] produces a comparable result in regions with heavy hazes. However, to overcome the depth jumps, the use of Laplacian matting is time consuming. There exists many depth jumps in the transmission. In this work, the background light or ambient light is simply calculated by the 0.1% of brightest pixels values, which incurred the results containing also some hazes.

Gibson et al.'s wiener filter based approach [26] can automatically refine the transmission by a locally adaptive wiener filter. This method also can be implemented for real time. However, it estimates the ambient light by a dark channel prior. It may cause the unpleasing result. The results also contain some hazes. Our transmission is much clear in the last row of Figure 5.

(a)   (b)

(c)   (d)
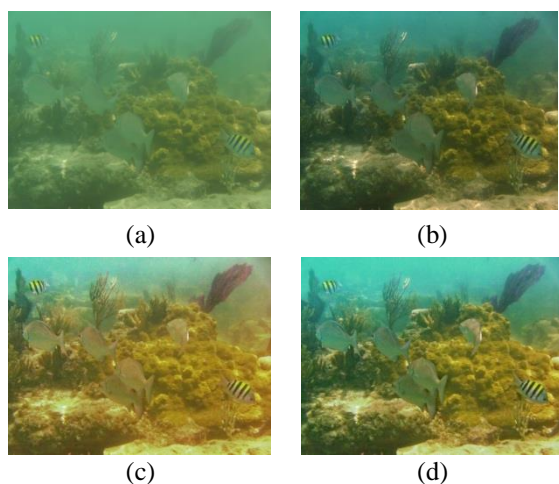
Figure 5: Results of different methods. (a) Input image. (b) He et al.'s method. (c) Gibson et al.'s method. (d) Our method.
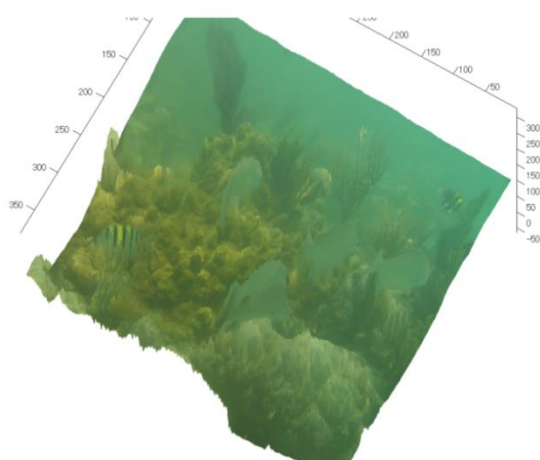
Figure 6: Reconstructed 3D underwater scene.

5. Conclusions

In this paper, we have explored and implemented novel image enhancement techniques for the shallow water optical image reconstruction. We have proposed a simple prior based on the difference in attenuation among the different color channels, which inspired us to estimate the transmission depth map. Another contribution compensated the transmission by a weighted guided trigonometric bilateral filter, which has the benefits of edge-preserving, noise removing, and the reduction in the computation time. Moreover, the proposed spectral-based underwater image colorization method successfully created colorful underwater distorted images that are better than the state-of-the-art methods. Furthermore, the reconstructed 3d scene is well performed.

Acknowledgments

References

[1]. D.M. Kocak; F.R. Dalgleish; F.M. Caimi; Y.Y. Schechner. A focus on recent developments and trends in underwater imaging. Mar. Technol. Soc. J., 42(1), 52–67, 2008.

[2]. R. Schettini; S. Corchs. Underwater image processing: state of the art of restoration and image enhancement methods. EURASIP J. Adv. Sig. Pr., 746052, 2010.

[3]. Y.Y. Schechner; Y. Averbuch. Regularized image recovery in scattering media. IEEE T. Pattern Anal., 29(9), 1655–1660, 2007.

[4]. C. Ancuti; C.O. Ancuti; T. Haber; P. Bekaert. Enhancing underwater images and videos by fusion. In Proceedings of IEEE Conference on Computer Vision and Pattern Recognition, 81–88, 2012.

[5]. W. Hou; D.J. Gray; A.D. Weidemann; G.R. Fournier; J.L. Forand. Automated underwater image restoration and retrieval of related optical properties. In Proceedings of IEEE International Symposium of Geoscience and Remote Sensing, 1889–1892, 2007.

[6]. B. Ouyang; F.R. Dalgleish; F.M. Caimi; A.K. Vuorenkoski; T.E. Giddings; J.J. Shirron. Image enhancement for underwater pulsed laser line scan imaging system. In Proceedings of SPIE, 8372, 83720R, 2012.

[7]. T. Treibitz; Y.Y. Schechner. Turbid scene enhancement using multi-directional illumination fusion. IEEE T. Image Process., 21(11), 4662–4667, 2012.

[8]. R. Fattal. Signal image dehazing. In SIGGRAPH, 1–9, 2008.

[9]. K. He; J. Sun; X. Tang. Single image haze removal using dark channel prior. IEEE T. Pattern Anal., 33(12), 2341–2353, 2011.

[10]. K. He; J. Sun; X. Tang. Guided image filtering. In Proceedings of the 11th European Conference on Computer Vision, 1, 1-14, 2010.

[11]. C. Tomasi; R. Manduchi. Bilateral filtering for gray and color images. In Proceedings of IEEE International Conference on Computer Vision, 839–846, 1998.

[12]. K.N. Chaudhury; D. Sage; M. Unser. Fast O(1) bilateral filtering using trigonometric range kernels. IEEE T. Image Process., 20(12), 3376–3382, 2011.

[13]. A. Rizzi; C. Gatta; D. Marini. A new algorithm for unsupervised global and local color correction. Pattern Recogn. Lett., 24, 1663–1677, 2003.

[14]. M. Chambah; D. Semani; A. Renouf; P. Courtellemont; A. Rizzi. Underwater color constancy: enhancement of automatic live fish recognition. In Proceedings of SPIE, 5293, 157–168, 2004.

[15]. M. Bertalmio; V. Caselles; E. Provenzi; A. Rizzi. Perceptual color correction through variational techniques. IEEE T. Image Process., 16(4), 1058–1072, 2007.

[16]. J. Tarel; N. Hautiere. Fast visibility restoration from a single color or gray level image. In Proceedings of IEEE Conference of Computer Vision and Pattern Recognition, 2201–2208, 2009.

[17]. C. Xiao; J. Gan. Fast image dehazing using guided joint bilateral filter. Visual Comput., 28(6–8), 713–721, 2012.

[18]. R. Mantiuk; K.J. Kim; A.G. Rempel; W. Heidrich. HDR-VDP2: a calibrated visual metric for visibility and quality predictions in all luminance conditions. ACM T. Graphic., 30(4), 40–52, 2011.

[19]. J.Y. Chiang; Y.C. Chen. Underwater image enhancement by wavelength compensation and dehazing. IEEE T. Image Process., 21(4), 1756–1769, 2012.

[20]. S. Bazeille; I. Quidu; L. Jaulin; J.P. Malkasse. Automatic underwater image pre-processing. In Proceedings of Caracterisation Du Milieu Marin, 1-8, 2006.

[21]. C-B Nicholas; M. Anush; R.M. Eustice. Initial results in underwater single image dehazing. In Proceedings of IEEE OCEANS, 1-8, 2010.

[22]. http://www.ni.com/white-paper/13306/en/

[23]. Z. Wang; A. C. Bovik; H. R. Sheikh; E. P. Simoncelli. Image quality assessment: from error measurement to structural similarity. IEEE T. Image Process., 13(1), 600-612, 2004.

[24]. J.M. Morel; A. B. Petro; C. Sbert. Fast implementation of color constancy algorithms. In Proceedings of SPIE, 7241, 724106, 2009.

[25]. S. Serikawa; H. Lu. Underwater image dehazing using joint trilateral filter. Comput. Elec. En., 41(1), 41-50, 2014.

[26]. ITU-R-BT.500-11, Methodology for the subjective assessment of the quality of television pictures, 2002.

[27]. H. Lu; Y. Li; S. Serikawa. Underwater image enhancement using guided trigonometric bilateral filter and fast automatic color correction. In Proceedings of IEEE International Conference on Image Processing, 3412-3416, 2013.

[28]. K. Sooknanan; A. Kokaram; D. Corrigan. Improving underwater visibility using vignetting correction. In Proceedings of SPIE, pp.83050M-1-8, 2012.

[29]. Y. Zheng; S. Lin; S.B. Kang; R. Xiao; J.C. Gee; C. Kambhamettu. Single-image vignetting correction from gradient distribution symmetries. IEEE T. Pattern Anal., 35(6), pp.1480-1494, 2013.

[30]. D.L. Bongiorno; M. Bryson; D.G. Dansereau; S.B. Williams. Spectral characterization of COTS RGB cameras using a linear variable edge filter. In Proceedings of SPIE-IS&T, vol.86600N, 2013.

[31]. M. Roser, M. Dunbabin, A. Geiger. Simultaneous underwater visibility assessment, enhancement and improved stereo. In Proceedings of ICRA, pp.1-8, 2014.

[32]. H. Hirschmueller. Stereo processing by semiglobal matching and mutual information. IEEE Transactions on Pattern Analysis and Machine Intelligence, 30(2), 328-341, 2008.

Huimin Lu received a B.S. degree in Electronics Information Science and Technology from Yangzhou University in 2008. He received M.S. degrees in Electrical Engineering from Kyushu Institute of Technology and Yangzhou University in 2011. He received a Ph.D. degree in Electrical Engineering from Kyushu Institute of Technology in 2014. Currently, he is a postdoctoral researcher and JSPS fellow at Kyushu Institute of Technology. His current research interests include computer vision, communication, and ocean information processing.

Yujie Li received the B.S. degree in Computer Science and Technology from Yangzhou University in 2009. And he received M.S. degrees in Electrical Engineering from Kyushu Institute of Technology and Yangzhou University in 2012, respectively. Recently, he is a Ph.D student in Kyushu Institute of Technology. Her research interests include computer vision, data mining, and image segmentation.

Xuelong Hu received the B.S. degree in Electronics Information Science and Technology from Southeast University in 1978, 1993, respectively. During 1978-1990, he was an assistant Professor in Yangzhou University. From 2003 to 2006, he was an associate Professor in Yangzhou University. Science 2006, he has been a Professor in Yangzhou University. Recently, he is the Director of Yangzhou University Computer Information Center. His current research interests include computer vision, image processing, Internet of Things.